

# Parsec-scale Imaging of the Radio-bubble Seyfert galaxy NGC 6764

P. Kharb

*Department of Physics, Rochester Institute of Technology, Rochester, NY 14623, USA*

`kharb@cis.rit.edu`

Ananda Hota

*Institute of Astronomy and Astrophysics, Academia Sinica, Taiwan*

J. H. Croston

*School of Physics and Astronomy, University of Southampton, UK*

M. J. Hardcastle

*Centre for Astrophysics Research, University of Hertfordshire, UK*

C. P. O'Dea

*Department of Physics, Rochester Institute of Technology, Rochester, NY 14623*

R. P. Kraft

*Harvard Smithsonian Center for Astrophysics, 60 Garden St, Cambridge, MA, USA*

D. J. Axon

*Department of Physics, Rochester Institute of Technology, Rochester, NY 14623*

*Department of Physics and Astronomy, University of Sussex, UK*

and

A. Robinson

*Department of Physics, Rochester Institute of Technology, Rochester, NY 14623*

## ABSTRACT

We have observed the composite active galactic nucleus (AGN)-starburst galaxy NGC 6764 with the Very Long Baseline Array at 1.6 and 4.9 GHz. These observations have detected a “core-jet” structure and a *possible* weak counterjet component at 1.6 GHz. The upper limits to the core and jet (1.6–4.9 GHz) spectral index are 0.6 and 0.3, respectively. Taken together with the high brightness temperature of  $\sim 10^7$  K for the core region, the radio emission appears to be coming from a synchrotron jet. At a position angle of  $\sim 25^\circ$ , the parsec-scale jet seems to be pointing closely toward the western edge of the southern kpc-scale bubble in NGC 6764. A real connection between the parsec- and sub-kpc-scale emission would not only suggest the presence of a curved jet, but also a close link between the AGN jet and the radio bubbles in NGC 6764. We demonstrate that a precessing jet model can explain the radio morphology from parsec- to sub-kpc scales, and the model best-fit parameters of jet speed and orientation are fully consistent with the observed jet-to-counterjet surface brightness ratio. The jet however appears to be disrupted on scales of hundreds of parsecs, possibly due to interaction with, and entrainment of the interstellar medium gas, which subsequently leads to the formation of bubbles. The jet energetics in NGC 6764 suggest that it would take 12–21 Myr to inflate the (southern) bubble. This timescale corresponds roughly to the starburst episode that took place in NGC 6764 about 15–50 Myr ago, and could be indicative of a close connection between jet formation and the starburst activity in this galaxy.

*Subject headings:* galaxies: individual (NGC 6764) — galaxies: jets — galaxies: Seyfert — techniques: interferometric — radio continuum

## 1. Introduction

Radio emission in Seyfert galaxies comes typically from weak outflows emanating from the active galactic nucleus (AGN), which appear to be emitted in random directions with respect to the host galaxy plane (Kinney et al. 2000; Gallimore et al. 2006). While the outflows in some Seyfert galaxies can extend to sub-kpc or even kpc-scales (Ulvestad & Wilson 1984; Baum et al. 1993; Colbert et al. 1996), they are rarely in the form of the type of collimated (100-)kpc-scale jets that are observed in radio-loud AGNs. Sensitive radio observations have, however, revealed the presence of bubble-like structures in some Seyfert galaxies (Elmouttie et al. 1995; Irwin & Saikia 2003; Hota & Saikia 2006; Kharb et al. 2006). While starburst-driven superwinds have been invoked to explain the radio bubbles in Seyferts (e.g., Baum et al. 1993), an AGN-related origin has been favored by other studies (Hota & Saikia

2006; Wilson 1981; Wehrle & Morris 1988; Taylor et al. 1992). Copious amounts of X-ray emission, usually explained as thermal radiation from hot gas, are found to be closely associated with the largely non-thermal radio emission (Cecil et al. 1995; Wilson et al. 2001; Croston et al. 2008). The complex radio and X-ray morphologies observed in Seyfert galaxies suggest that the emission may come from a number of different, yet closely related, mechanisms.

On parsec scales, Very Long Baseline Interferometry (VLBI) observations typically reveal weak radio “cores” and “jet-like” extensions in Seyfert galaxies (Middelberg et al. 2004). While Doppler boosting of emission has been invoked in a few Seyfert jets (e.g., Mrk 231; Reynolds et al. 2009), Seyfert jets are normally sub-relativistic (Ulvestad et al. 1998). A link between star formation and Seyfert nuclear activity has often been suggested (e.g., Weedman 1983; Davies et al. 2007). On account of the faintness of the AGN emission, contributions from nuclear starbursts can become significant, thereby confusing the exact origin of the radio emission in Seyfert galaxies.

NGC 6764 is a nearby ( $z=0.00806^1$ , luminosity distance = 32.2 Mpc) barred spiral galaxy (type SB(s)bc), alternatively classified as a LINER, a Seyfert 2, and a Wolf-Rayet galaxy (one with signatures of recent massive star formation). Kiloparsec-scale radio observations with the Very Large Array (VLA) and the Giant Meterwave Radio Telescope (GMRT) have revealed  $\sim 1$  kpc (total extent  $\sim 2.6$  kpc) north-south (N-S) orientated bipolar bubbles of non-thermal radio emission along the minor axis of the spiral host galaxy (Hota & Saikia 2006). In addition, the higher resolution 5 GHz and 8 GHz VLA A-array configuration images of Hota & Saikia (2006) show a region of bright radio emission extending roughly in the east-west (E-W) direction.

The *ROSAT* X-ray Observatory detected a highly variable X-ray source in NGC 6764, which pointed to the presence of a compact, actively accreting AGN (Schinnerer et al. 2000). Recent *Chandra* X-ray observations of NGC 6764 have discovered extended X-ray emission, well coincident with the N-S orientated radio bubbles (Croston et al. 2008). Bright X-ray emission is also observed in the E-W region coincident with the high surface brightness radio emission. X-ray spectral fitting of the N-S bubbles has shown that the X-ray data are best fitted by a hot thermal gas model with  $kT = 0.75$  keV, while the E-W extension is best fitted by hot thermal gas plus absorption with  $kT = 0.93$  keV and  $N_H = 2 \times 10^{21}$  cm $^{-2}$ . The total energy stored in the hot gas is high ( $\sim 10^{56}$  erg), and cannot be ascribed to a nuclear starburst alone; an AGN-related origin appears much more likely (see Croston et al. 2008).

---

<sup>1</sup>At the distance of NGC 6764,  $1''$  corresponds to 154 pc, for  $H_0 = 71$  km s $^{-1}$  Mpc $^{-1}$ ,  $\Omega_{mat} = 0.27$ , and  $\Omega_{vac} = 0.73$ .

The X-ray hardness ratio maps (using the 1.0–5.0 keV and 0.4–1.0 keV filtered images) indicate that the western edge of the kpc-scale bubbles has a relatively hard X-ray spectrum. Radio spectral index maps (using the 1.4–4.9 GHz VLA and the 1.4–8.4 GHz VLA and GMRT images) revealed the south-western edge to have a flatter radio spectrum (see Hota & Saikia 2006). The radio and X-ray spectral flattening could be signifying enhanced localized particle reacceleration along the south-western edge of the bubbles. The radio–X-ray results strongly support a scenario wherein an AGN outflow is shock heating and entraining the warm interstellar medium (ISM) gas in the south-western region of the bubble. However, the jet direction could not be unambiguously determined from the kpc-scale radio observations (Hota & Saikia 2006), leading to some confusion about how the radio/X-ray bubbles were powered by the AGN. In order to resolve this issue, we observed NGC 6764 with the Very Long Baseline Array (VLBA) at 1.6 and 4.9 GHz, and we report the results of these observations in this paper.

## 2. VLBA Observations

We observed NGC 6764 with the ten elements of the VLBA (Napier et al. 1994) on 2008 November 13, at 4.9 and 1.6 GHz (Project ID BK154), in a phase-referencing experiment (Beasley & Conway 1995). The calibrator 1758+388 was used as the fringe-finder, while the compact source 1917+495 with a switching angle of  $2^\circ$  and an X, Y, positional error of 0.38, 0.70 *mas*, respectively, was chosen as the phase reference calibrator<sup>2</sup>. A switching cycle of 5 minutes (calibrator 2 minutes and target 3 minutes) was adopted at both the frequencies. The calibrator 1924+507 ( $\sim 2.8^\circ$  away and with a high positional accuracy) was used as the phase check source. A phase check source could be used to get a measure of the decorrelation expected on the target, in the case of a non-detection.

The observations<sup>3</sup> were made using the standard setup with 128 Mbps recording and a 2-bit sampling rate, with two 8 MHz intermediate frequency channels (IFs) in dual polarization. This yielded a total bandwidth of  $(8 \times 2 \times 2 =) 32$  MHz. We followed the standard VLBA data reduction procedures using the NRAO Astronomical Image Processing System (AIPS, Greisen 2003) as described in Appendix C of the AIPS Cookbook. Delays were corrected using fringe fitting on the fringe finder (with AIPS task FRING). The phase calibrator 1917+495 was iteratively imaged and self-calibrated using the AIPS tasks IMAGR and CALIB. The images were then used as models to determine the amplitude and phase

---

<sup>2</sup>See <http://www.vlba.nrao.edu/astro/calib/>

<sup>3</sup><http://www.vlba.nrao.edu/astro/VOBS/astronomy/nov08/bk154/>

gains for the antennas. These gains were applied to the target and phase check source, and images were made using IMAGR. Due to the faintness of the source, self-calibration was not possible (there were too many failed solutions). The total on-source time was  $\sim 120$  minutes at 1.6 GHz, and  $\sim 150$  minutes at 4.9 GHz, which resulted in a final *rms* noise of  $\sim 90 \mu\text{Jy beam}^{-1}$  at 1.6 GHz, and  $\sim 80 \mu\text{Jy beam}^{-1}$  at 4.9 GHz. The images displayed in Figure 1 were created with uniform weighting (with ROBUST 0 in IMAGR for 1.6 GHz, and ROBUST 5, UVTAPER 0 – 70  $\text{M}\lambda$  for 4.9 GHz). The insets display the elliptical Gaussian beams with dimensions =  $7.7 \text{ mas} \times 5.7 \text{ mas}$ , at a position angle (PA) of  $-31^\circ$  for 1.6 GHz, and  $3.6 \text{ mas} \times 3.0 \text{ mas}$  at a PA of  $-13^\circ$  for 4.9 GHz.

### 3. Results

We have detected two distinct radio components at 1.6 GHz (marked 1 and 2 in Figure 1). There is a suggestion of a weak third component to the north of component 1. New sensitive radio observations are required to confirm this feature. The source position is  $\sim 0.58''$  away from the listed optical host galaxy position of R.A. 19h 08m 16.370s, decl. 50d 55m 59.58s (Clements 1981). We identify components 1, 2 and 3 to be the core, the jet, and a *possible* counterjet, respectively. The “core-jet” structure extends to  $\sim 0.8$  parsec, at a P.A. of  $\sim 25^\circ$ . The peak surface brightness of the core, and the total radio flux density of the “core-jet” structure are  $0.46 \text{ mJy beam}^{-1}$  and  $0.80 \text{ mJy}$ , respectively. The peak intensities and positions of the radio components, estimated using AIPS tasks JMFIT and IMDIST, are listed in Table 1.

In order to test the credibility of component 3, we estimated a surface density of spurious noise peaks in the image by dividing the number of noise peaks having a signal-to-noise ratio (S/N) similar to component 3 (*i.e.*,  $\text{S/N} > 2.6$ ), by the entire image. We found around 230 noise peaks in an image of size  $0.4'' \times 0.4''$ , resulting in a noise peak surface density of  $\sim 1370$  peaks  $\text{arcsec}^{-2}$ . Considering then a region of size ( $15 \text{ mas} \times 15 \text{ mas}$ ), centered around the peak source emission, as the region where a noise peak could be mistaken for source emission (the core-jet distance being  $\sim 5 \text{ mas}$ ), we estimated that 0.3 noise peaks could be expected in this region. Therefore, there is a 30% chance that component 3 is a noise peak.

The 1.4 GHz peak flux density of the VLA A-array core (size  $\sim 1.5''$ ) is  $\sim 14 \text{ mJy}$  (Hota & Saikia 2006). This implies that only about 6% of the VLA flux density is detected by the VLBA. This is similar to what is observed in the Seyfert galaxy NGC 4151 ( $\sim 8\%$ ; Pedlar et al. 1993; Ulvestad et al. 1998). We believe, however, that had self-calibration worked in NGC 6764, its fraction of VLBA to VLA flux density would have been higher. Nevertheless, it appears that there is either a lot of diffuse emission on scales of tens or

hundreds of parsecs which are not visible to the VLBA, or the VLBA is not sensitive to the diffuse radio emission on parsec scales (this appears to be less likely in the case of NGC 6764 considering the large fraction of missing flux), or a combination of both (see Orienti & Prieto 2010 for a discussion on the missing diffuse emission in VLBI observations).

There appears to be a tentative detection of components 1 and 2 at 4.9 GHz. However, this detection is also in need of new confirmatory observations, as the radio peak in components 1 and 2 is only around 3 times the *rms* noise ( $\sim 80 \mu\text{Jy beam}^{-1}$ ), while the total flux density is only  $\sim 0.3 \text{ mJy}$ . As the 4.9 GHz emission is weak, we have not attempted to create a spectral index map. Using the  $3 \times \textit{rms}$  value from the 4.9 GHz map, we estimate upper limits to the spectral indices (defined such that  $S_\nu \propto \nu^{-\alpha}$ , where  $S_\nu$  is the flux density at frequency  $\nu$ ). These are  $> 0.6$  and  $> 0.3$  for components 1 and 2, respectively.

The steep radio spectrum of the radio core is consistent with many Seyfert core observations in the literature (e.g., Sadler et al. 1995; Roy et al. 2000; Orienti & Prieto 2010), and suggests optically-thin synchrotron emission. The steep radio spectrum of the radio core rules out thermal free-free radiation as the dominant emission mechanism. The brightness temperature of the radio emission ( $T_B$ ) can be estimated using the relation,  $T_B = 1.8 \times 10^9 (1+z) (\frac{S_\nu}{1 \text{ mJy}}) (\frac{\nu}{1 \text{ GHz}})^{-2} (\frac{\theta_1 \theta_2}{2 \text{ mas}^2})^{-1} \text{ K}$ , where  $z$  is the redshift,  $\theta_1, \theta_2$  are, respectively, the major and minor axes of the beam, and the factor  $1/2$  arises for the case of “unresolved” components (Ulvestad et al. 2005). For a core region of size (= beam-size)  $= 7.7 \text{ mas} \times 5.7 \text{ mas}$ , the brightness temperature is of the order of  $1.5 \times 10^7 \text{ K}$ . This is consistent with the brightness temperatures observed in other Seyfert nuclei (Kukula et al. 1999; Middelberg et al. 2004; Orienti & Prieto 2010). The high brightness temperature provides further support to a non-thermal origin of the radio emission. We note that starburst galaxies typically exhibit brightness temperatures of  $< 10^5 \text{ K}$  (Condon et al. 1991).

#### 4. Discussion

At a P.A. of  $\sim 25^\circ$ , the parsec-scale jet is pointing closely to the western edge of the southern kpc-scale radio bubble. This region (marked “A” in the top panel of Figure 2) has a flatter radio and a harder X-ray spectrum (Hota & Saikia 2006; Croston et al. 2008). The VLBA jet appears to be in the same direction as the weak jet-like extension observed in the high-resolution VLA (A-array, 8 GHz) observations, which is marked “Jet?” in Figure 11 of Hota & Saikia (2006) and in the middle panel of Figure 2. A connection between the radio emission on parsec- and sub-kpc scales in NGC 6764 would require the jet to be curved. While this connection needs to be examined in greater detail with more sensitive sub-kpc resolution (e.g., 5 GHz EVLA A-array) radio observations, bent or S-shaped radio

jets have often been observed in Seyfert galaxies (e.g., Kukula et al. 1995; Nagar et al. 1999; Thean et al. 2000). Three popular scenarios for jet bending have been expounded: (1) precession of the jet “nozzle” in the galactic nucleus (Ekers et al. 1978), (2) ram-pressure of the rotating ISM (Wilson & Ulvestad 1982), and (3) static pressure gradients in the hot gaseous galactic halo (Smith & Norman 1981). However, a combination of these and possibly other effects (like starburst superwinds bending the slow radio jets, as suggested for NGC 6764 by Hota & Saikia (2006)) could all be in play here, to varying extents. It is also feasible that the misaligned VLBI jet is a new jet which has little to do with the N-S bubbles, which are in turn, just relic emission from a previous activity episode. We briefly explore these ideas ahead.

#### 4.1. Precessing Jet and Bubbles

Precessing radio jets have been directly observed in Galactic X-ray binaries (e.g., Mioduszewski et al. 2001) and suggested to be present in Seyfert galaxies with curved jets like NGC 3516 (Veilleux et al. 1993). The detection of two pairs of orthogonally-placed, self-similar edge-brightened radio bubbles in the Seyfert galaxy Mrk 6, prompted Kharb et al. (2006) to invoke two episodes of precessing radio jets to explain the radio structures. Jet precession could arise due to the presence of binary black holes (Caproni & Abraham 2004), the relativistic Lense-Thirring effect (Bardeen & Petterson 1975; Caproni et al. 2006), or accretion disk warping due to non-axisymmetric radiation pressure forces (Pringle 1996). The Seyfert galaxy Circinus has radio bubbles with bright, highly polarized edges (Elmouttie et al. 1995), similar to the “edge-brightened” Mrk 6 and NGC 6764, and a precessing accretion disk, as evidenced by the VLBI water maser observations of Greenhill et al. (2003). A precessing disk and S-shaped radio jets with tightly correlated X-ray emission have also been observed in the Seyfert galaxy NGC 4258 (Sanders 1982; Cecil et al. 2000; Wilson et al. 2001). Therefore, the presence of a precessing jet in the radio-bubble galaxy, NGC 6764, is a viable possibility.

Hjellming & Johnston (1981) presented a three-dimensional kinematic model to explain the proper motions of the precessing jet in the X-ray binary SS433. This model has since been successfully applied to the radio morphologies of radio-powerful AGNs (e.g., Gower et al. 1982). Following the relations in Hjellming & Johnston (1981), we have attempted to fit a precessing jet model to the radio structure in NGC 6764. We find that this model is able to fit the radio structure from parsec to sub-kpc scales (see Figure 2). The best-fit model parameters are: jet speed =  $0.028c$ , jet P.A. =  $76^\circ$ , inclination =  $18^\circ$ , precession cone half-opening angle =  $3^\circ$ , and angular velocity =  $1.4 \times 10^{-5} \text{ rad yr}^{-1}$ . Apart from the radio morphology, this model is consistent with a couple of different observational findings. In

the top panel of Figure 2, “A” marks the region with the flatter radio and harder X-ray spectrum, while “B” marks the location of a prominent, curved  $H\alpha$  filament (Zurita et al. 2000; Hota & Saikia 2006; Leon et al. 2007), seen here as coincident with the precessing radio counterjet. Hota & Saikia (2006) were the first to present and discuss the radio– $H\alpha$  image overlays. The correspondence of the jet with these regions can explain both the spectral flattening in the south (particle re-acceleration) and emission lines in the north (shock excitation). Clearly, this study would greatly benefit from (shock-sensitive) [NII]/ $H\alpha$  emission line observations of NGC 6764 (e.g., Sharp & Bland-Hawthorn 2010).

While keeping in mind the uncertainties involved in the surface brightness values of the faint detected features, we estimated the observed jet-to-counterjet surface brightness ratio ( $R_j$ ) at three positions along the jet and counterjet. We note that if component 3 is a noise peak, then the  $R_j$  estimates above must be regarded as lower limits. Taking the peak surface brightness values of components 2 (jet) and 3 (counterjet), we derive an  $R_j \sim 1.5$ . However, the peak positions of components 2 and 3 are not equidistant from the peak of component 1 (core). Therefore, taking the peak position of component 2 as a reference, we obtained the surface brightness at a distance of  $\sim 4.5$  mas from the core (this being the distance between components 1 and 2) in the counterjet direction. This resulted in  $R_j \sim 1.9$ . Similarly, taking the peak position of component 3 as a reference, we obtained the surface brightness value at a distance of  $\sim 6$  mas from the core (the distance between components 1 and 3) in the jet direction. This yielded an  $R_j \sim 1.2$ . This latter value is perhaps the more robust among the three estimates, as it relies on the “peak” surface brightness of the weak component 3, rather than on the noise around it (as was used to get  $R_j \sim 1.9$ ). This  $R_j$  value of  $\sim 1.2$  matches closely with the expected jet-to-counterjet ratio ( $R_j = (\frac{1+\beta \cos \theta}{1-\beta \cos \theta})^p$ ) of  $\sim 1.15$ , for a Doppler-boosted radio jet with speed  $0.028c$  and an inclination of  $18^\circ$  (both precessing jet model best-fit parameters) for a jet structural parameter of  $p \approx 2 + \alpha = 2.6$  (e.g., Urry & Padovani 1995). Therefore, the current parsec-scale data on NGC 6764 are *not inconsistent* with a precessing jet model. It is important to note that the half-opening angle of the precession cone is only  $3^\circ$ , which implies that the jet is very gently curved. Low-pitch precessing jets have been proposed for radio-loud AGNs as well (Conway & Murphy 1993; Kharb et al. 2010).

However, there are potential difficulties in proposing a precessing jet model similar to that proposed in Mrk 6 by Kharb et al. (2006), for NGC 6764. In Kharb et al., we attempted to explain the entire edge-brightened bubble with the highly polarized edges, as the projection of a collimated precessing jet. This picture has definite shortcomings in the case of NGC 6764. As noted previously, while part “B” of the (counter-) jet in Figure 2 may be coincident with a curved  $H\alpha$  filament, indicative of the ionized hydrogen gas; there is no clear evidence of a jet-like extension in the region marked “A” in the top panel of Figure 2,



beyond what is observed in the middle panel of Figure 2. The major clue to the presence of a jet there, are the flatter radio and harder X-ray spectra. Moreover, the  $H\alpha$  image in Zurita et al. (2000) shows other bright curved filaments, notably toward the south-eastern edge of the bubble, where a precessing jet model (with the same best-fit parameters as above) cannot be fitted. Lastly, a shock, rather than a collimated jet, could also produce the flatter radio and harder X-ray spectra.

Recent X-ray observations of central galaxies in clusters have indicated multiple X-ray cavities in some of them (e.g., Perseus A, NGC 5813, A2626). The connection of these, sometimes non-collinear cavities, with the bent radio jets has suggested the picture of a precessing jet, or a jet that changes direction, inflating bubbles at multiple epochs (see Dunn et al. 2006; Wong et al. 2008; Falceta-Gonçalves et al. 2010; Randall et al. 2010). It is also possible, however, that the apparent differences in the direction are due to the dynamics of the intracluster medium. Sternberg & Soker (2008) have suggested that slow jets with larger opening angles could give rise to fat bubbles. Therefore, although the picture of precessing jets inflating bubbles and creating X-ray cavities in powerful cluster radio galaxies is yet to be fully established, it is tantalizing to suggest that a similar process could be taking place in Seyferts which have radio bubbles. This then suggests an intimate connection between radio bubbles and radio jets, and leads us naturally to the next topic of jet-ISM interaction and the inflation of bubbles.

## 4.2. Jet-ISM Interaction and Bubbles

As the entire radio emission in NGC 6764 cannot be fitted with a precessing or curved radio jet, disruption or de-collimation due to a strong interaction with the ISM or winds, from either the starburst or AGN, is indicated. As mentioned earlier, there is some evidence for direct interaction between the jet and the X-ray emitting plasma close to the nucleus. Ram pressure bending due to a rotating ISM could also give rise to the jet curvature itself. Following an approach similar to Wilson & Ulvestad (1982), we tried to deduce if the radio jet in NGC 6764 bends in the correct sense, if it was indeed a result of jet–rotating-ISM interaction. Assuming that the spiral arms “trail” in spiral galaxies (e.g., de Vaucouleurs 1958), we see that NGC 6764 must rotate counter-clockwise. Then the VLBA jet, at least, seems to “lead” the rotation of the galaxy and therefore, could be interacting with the rotating gas (see the bottom panel of Figure 2), although a possible problem for this model is that the jet on scales larger than that probed by the VLBA (as in the middle panel of Figure 2) would be moving in the opposite direction and against the rotating medium. Furthermore, the kpc-scale bubbles should be carried downstream in the direction of the

rotating medium, which is not observed. Therefore, the jet–rotating-ISM argument becomes weak in NGC 6764.

An alternative model that can explain the absence of a collimated jet on sub-kpc scales is one in which the initially SW-NE jet strongly interacts with cold, dense material in the host galaxy (e.g., Leon et al. 2007; Middelberg et al. 2007), and is disrupted, giving rise to pressure-driven bubbles (perhaps containing hot thermal material) which expand to the north and south. The physics behind this phenomenon is that entrainment of cold material simultaneously reduces the bulk speed of the jet and increases (via dissipation) the internal energy density (e.g., Begelman 1982). Once the bulk speed of the jet is of the order of the transverse expansion speed driven by the internal energy density, one no longer has a jet, but a bubble. The bubbles would sweep up the gas at the leading edge and result in edge-brightening (due to increased thermal free-free emission), as is observed in NGC 6764.

One observational clue that might in principle go against the idea of bubbles sweeping up the gas, is that the X-ray emission in NGC 6764 seems to be fully coincident with the radio emission (as is also observed in other Seyfert galaxies; see Cecil et al. 1995; Veilleux & Bland-Hawthorn 1997; Wilson et al. 2000). An expanding superbubble should be accompanied by extended X-ray emission from hot gas, but not from the cooler shell, which should just exhibit  $H\alpha$  emission. For the swept-up gas ahead of the shock-front that is ionized, the X-ray emission should be ahead of the radio emission.

### 4.3. Energetics

Under the assumption of “equipartition” of energy between relativistic particles and the magnetic field (Burbidge 1959; Miley 1980), we estimated the magnetic field strength and other parameters for a cylindrical jet geometry. The total radio luminosity was estimated assuming that the radio spectrum extends from 10 MHz to 100 GHz with a spectral index of  $\alpha=0.6$ . Further, it was assumed that the relativistic protons and electrons have equal energies, and the radio emitting plasma has a volume filling factor of unity. From the 1.6 GHz image, we estimate the size of the radio jet to be  $11.8\ mas \times 8.1\ mas$ . Following the relations in O’Dea & Owen (1987), we obtain a total radio luminosity of  $\sim 2.4 \times 10^{37}\ erg\ s^{-1}$ , minimum magnetic field ( $B_{min}$ ) of  $\sim 1.26\ mG$ , minimum energy of  $\sim 2.1 \times 10^{49}\ erg$ , and a minimum pressure ( $P_{min}$ ) of  $\sim 1.5 \times 10^{-7}\ dynes\ cm^{-2}$ .

The electron lifetime due to synchrotron radiative losses can be estimated using the relation,  $t_{syn} \simeq 33.4\ B_{10}^{-3/2}\ \nu_c^{-1/2}\ Myr$ , where  $B_{10}$  is the magnetic field (“minimum”  $B$  field here) in units of  $10\ \mu G$ , and  $\nu_c$  is the critical frequency in GHz (e.g., Pacholczyk 1970).

This turns out to be  $\sim 1.8 \times 10^4$  yrs for a critical frequency of 1.6 GHz. Assuming that the radio jet is being confined by, and is in pressure balance with the surrounding ISM gas (*i.e.*,  $P_{min} = nk_B T$ ), we estimate that the gas at a temperature of 0.25 keV would need to have a density of  $\sim 400 \text{ cm}^{-3}$  in order to do so.

#### 4.4. The AGN Jet and Starburst connection

NGC 6764 is well understood to be a composite AGN-starburst system. From the *Chandra* X-ray observations of NGC 6764, Croston et al. (2008) have estimated the hot X-ray gas pressure of  $(4-7) \times 10^{-12} \text{ dynes cm}^{-2}$  in the southern bubble. If we assume that the radio jet does  $4PV$  work in order to inflate this bubble, then for a bubble volume of  $\sim 1.46 \times 1.16 \times 1.16 \text{ kpc}^3 = 1.93 \text{ kpc}^3$ , this turns out to be  $(9-16) \times 10^{53} \text{ ergs}$ , assuming that the gas inside and outside the bubble is in a pressure balance. Further assuming that the efficiency ( $\epsilon$ ) with which the total jet energy is tapped to produce radio luminosity is 1% (e.g., O’Dea 1985), the jet with a radio luminosity of  $2.4 \times 10^{37} \text{ erg s}^{-1}$  and a kinetic luminosity ( $L_{rad}/\epsilon$ ) of  $\sim 2.4 \times 10^{39} \text{ erg s}^{-1}$  would take 12–21 Myr to create the bubble. Interestingly, this timescale matches closely with a starburst activity episode in NGC 6764. Spectral synthesis models of Schinnerer et al. (2000) have suggested two major starburst episodes in the nuclear regions ( $\sim 3'' = 460 \text{ pc}$ ) that occurred 3–5 Myr and 15–50 Myr ago. If the timescales are indeed correlated, it could suggest that an accretion event about 10–20 Myr ago might have initiated a starburst, and eventually powered the AGN jet (e.g., Davies et al. 2007; Tremblay et al. 2010). This then would be a strong indicator of a close connection between AGN activity and violent nuclear star formation in a Seyfert galaxy.

The presence of non-thermal filaments in some Seyfert galaxies has been suggested to be the aftermath of burst superbubbles (e.g., Veilleux et al. 1993; Veilleux & Bland-Hawthorn 1997). However, the fact that very often these filaments seem to pass through the AGN core (e.g., NGC 3079; Cecil et al. 2001), suggests strongly that bubbles, if present, are linked to the AGN, rather than to starburst or galactic superwinds alone. The results presented in this paper clearly highlight the close connection between an AGN outflow and the kpc-scale radio bubble in yet another Seyfert galaxy, NGC 6764.

Finally, it is interesting to note that, using a sample of 60 warm infrared galaxies, Kewley et al. (2000) discovered a bimodal distribution in the compact 2.3 GHz radio luminosity: majority of the galaxies above and below a threshold 2.3 GHz luminosity of  $L_{2.3} \sim 1.7 \times 10^{21} \text{ W Hz}^{-1}$  were AGNs and starbursts, respectively. We find that the 2.3 GHz luminosity of NGC 6764, which is  $L_{2.3} \sim 5.3 \times 10^{19} \text{ W Hz}^{-1}$  (assuming a 1.6–2.3 GHz spectral index of 0.6), places it in the starburst category. However, the “core-jet” radio mor-

phology, and the high brightness temperature, strongly supports the presence of an AGN in NGC 6764.

## 5. Summary and Conclusions

1. We have observed the composite AGN-starburst galaxy NGC 6764 with the VLBA at 1.6 and 4.9 GHz. The VLBA observations clearly detect a “core-jet” structure with a *possible* weak counterjet component at 1.6 GHz. There is a tentative detection of the core and jet at 4.9 GHz, but it requires further confirmatory observations.
2. We derive upper limits to the 1.6–4.9 GHz radio spectral index for the core and jet, which are  $> 0.6$  and  $> 0.3$ , respectively. Taken along with the high brightness temperature of  $\sim 10^7$  K for the core region, this suggests that the radio emission comes from a synchrotron jet.
3. The parsec-scale jet, at a P.A. of  $\sim 25^\circ$ , appears to be pointing closely toward the region with the relatively flat radio and harder X-ray spectrum in the western edge of the southern bubble. A connection between the radio emission on parsec- and sub-kpc scales would indicate that the radio bubbles in NGC 6764 are indeed powered by an AGN jet. Furthermore, it would require the AGN jet to be curved.
4. We find that the curved (or misaligned) jet can be fitted with a precessing jet model from the parsec to sub-kpc scales. However, not all of the radio emission in NGC 6764 can be fitted by a precessing or curved radio jet, as was successfully modeled for Mrk 6. The jet appears to be disrupted beyond sub-kpc scales, possibly due to the loss of momentum by interaction and/or entrainment of the ISM, leading eventually to the creation of lobe-like bubbles. This is consistent with the copious X-ray emission observed co-spatial with the radio emission in NGC 6764 (Croston et al. 2008).
5. Following the suggestion of a compact-radio-luminosity dichotomy in AGNs and starbursts (Kewley et al. 2000), we find that even though the extrapolated 2.3 GHz luminosity of NGC 6764 ( $\sim 5 \times 10^{19}$  W Hz $^{-1}$ ) places it in the starburst category, the high brightness temperature and morphology strongly support the picture of an AGN in NGC 6764.
6. The jet energetics suggest that it would take 12–21 Myr for the jet to inflate the (southern) bubble. This timescale corresponds roughly to the starburst episode that took place in NGC 6764 about 15–50 Myr ago. This could point to a close connection between the ejection of the AGN jet and the starburst episode, which might have resulted from a common accretion event in the galaxy.

7. NGC 6764 seems to present a convincing example of an AGN jet that is closely associated with the kpc-scale radio bubbles. It is tantalizing to invoke a correspondence between this picture and that proposed for powerful cluster radio galaxies like Perseus A (e.g., Dunn et al. 2006; Falceta-Gonçalves et al. 2010).

We thank the referee for helpful suggestions which have improved this paper significantly. We acknowledge the technical help provided by Joan Wrobel in scheduling the VLBA observations. This work is partially supported by NASA grant G08-9108X. This research has made use of the NASA/IPAC Extragalactic Database (NED) which is operated by the Jet Propulsion Laboratory, California Institute of Technology, under contract with the National Aeronautics and Space Administration. M.J.H. thanks the Royal Society for support.

## REFERENCES

- Bardeen, J. M., & Petterson, J. A. 1975, *ApJ*, 195, L65
- Baum, S. A., O’Dea, C. P., Dallacassa, D., de Bruyn, A. G., & Pedlar, A. 1993, *ApJ*, 419, 553
- Beasley, A. J., & Conway, J. E. 1995, in *Astronomical Society of the Pacific Conference Series*, Vol. 82, *Very Long Baseline Interferometry and the VLBA*, ed. J. A. Zensus, P. J. Diamond, & P. J. Napier, 328
- Begelman, M. C. 1982, in *IAU Symposium*, Vol. 97, *Extragalactic Radio Sources*, ed. D. S. Heeschen & C. M. Wade, 223–225
- Burbidge, G. R. 1959, *ApJ*, 129, 849
- Caproni, A., & Abraham, Z. 2004, *ApJ*, 602, 625
- Caproni, A., Livio, M., Abraham, Z., & Mosquera Cuesta, H. J. 2006, *ApJ*, 653, 112
- Cecil, G., Bland-Hawthorn, J., Veilleux, S., & Filippenko, A. V. 2001, *ApJ*, 555, 338
- Cecil, G., Greenhill, L. J., DePree, C. G., Nagar, N., Wilson, A. S., Dopita, M. A., Pérez-Fournon, I., Argon, A. L., & Moran, J. M. 2000, *ApJ*, 536, 675
- Cecil, G., Wilson, A. S., & de Pree, C. 1995, *ApJ*, 440, 181
- Clements, E. D. 1981, *MNRAS*, 197, 829

- Colbert, E. J. M., Baum, S. A., Gallimore, J. F., O’Dea, C. P., & Christensen, J. A. 1996, *ApJ*, 467, 551
- Condon, J. J., Huang, Z., Yin, Q. F., & Thuan, T. X. 1991, *ApJ*, 378, 65
- Conway, J. E., & Murphy, D. W. 1993, *ApJ*, 411, 89
- Croston, J. H., Hardcastle, M. J., Kharb, P., Kraft, R. P., & Hota, A. 2008, *ApJ*, 688, 190
- Davies, R. I., Sánchez, F. M., Genzel, R., Tacconi, L. J., Hicks, E. K. S., Friedrich, S., & Sternberg, A. 2007, *ApJ*, 671, 1388
- de Vaucouleurs, G. 1958, *ApJ*, 127, 487
- Dunn, R. J. H., Fabian, A. C., & Sanders, J. S. 2006, *MNRAS*, 366, 758
- Ekers, R. D., Fanti, R., Lari, C., & Parma, P. 1978, *Nature*, 276, 588
- Elmouttie, E., Haynes, R. F., Jones, K. L., Ehle, M., Beck, R., & Wielebinski, R. 1995, *MNRAS*, 275, L53
- Falceta-Gonçalves, D., Caproni, A., Abraham, Z., Teixeira, D. M., & de Gouveia Dal Pino, E. M. 2010, *ApJ*, 713, L74
- Gallimore, J. F., Axon, D. J., O’Dea, C. P., Baum, S. A., & Pedlar, A. 2006, *AJ*, 132, 546
- Gower, A. C., Gregory, P. C., Unruh, W. G., & Hutchings, J. B. 1982, *ApJ*, 262, 478
- Greenhill, L. J., Booth, R. S., Ellingsen, S. P., Herrnstein, J. R., Jauncey, D. L., McCulloch, P. M., Moran, J. M., Norris, R. P., Reynolds, J. E., & Tzioumis, A. K. 2003, *ApJ*, 590, 162
- Greisen, E. W. 2003, in *Astrophysics and Space Science Library*, Vol. 285, *Astrophysics and Space Science Library*, ed. A. Heck, 109
- Hjellming, R. M., & Johnston, K. J. 1981, *ApJ*, 246, L141
- Hota, A., & Saikia, D. J. 2006, *MNRAS*, 371, 945
- Irwin, J. A., & Saikia, D. J. 2003, *MNRAS*, 346, 977
- Kewley, L. J., Heisler, C. A., Dopita, M. A., Sutherland, R., Norris, R. P., Reynolds, J., & Lumsden, S. 2000, *ApJ*, 530, 704
- Kharb, P., Lister, M. L., & Cooper, N. J. 2010, *ApJ*, 710, 764

- Kharb, P., O’Dea, C. P., Baum, S. A., Colbert, E. J. M., & Xu, C. 2006, *ApJ*, 652, 177
- Kinney, A. L., Schmitt, H. R., Clarke, C. J., Pringle, J. E., Ulvestad, J. S., & Antonucci, R. R. J. 2000, *ApJ*, 537, 152
- Kukula, M. J., Ghosh, T., Pedlar, A., & Schilizzi, R. T. 1999, *ApJ*, 518, 117
- Kukula, M. J., Pedlar, A., Baum, S. A., & O’Dea, C. P. 1995, *MNRAS*, 276, 1262
- Leon, S., Eckart, A., Laine, S., Kotilainen, J. K., Schinnerer, E., Lee, S., Krips, M., Reunanen, J., & Scharwächter, J. 2007, *A&A*, 473, 747
- Middelberg, E., Agudo, I., Roy, A. L., & Krichbaum, T. P. 2007, *MNRAS*, 377, 731
- Middelberg, E., Roy, A. L., Nagar, N. M., Krichbaum, T. P., Norris, R. P., Wilson, A. S., Falcke, H., Colbert, E. J. M., Witzel, A., & Fricke, K. J. 2004, *A&A*, 417, 925
- Miley, G. 1980, *ARA&A*, 18, 165
- Mioduszewski, A. J., Rupen, M. P., Hjellming, R. M., Pooley, G. G., & Waltman, E. B. 2001, *ApJ*, 553, 766
- Nagar, N. M., Wilson, A. S., Mulchaey, J. S., & Gallimore, J. F. 1999, *ApJS*, 120, 209
- Napier, P. J., Bagri, D. S., Clark, B. G., Rogers, A. E. E., Romney, J. D., Thompson, A. R., & Walker, R. C. 1994, *IEEE Proceedings*, 82, 658
- O’Dea, C. P. 1985, *ApJ*, 295, 80
- O’Dea, C. P., & Owen, F. N. 1987, *ApJ*, 316, 95
- Orienti, M., & Prieto, M. A. 2010, *MNRAS*, 401, 2599
- Pacholczyk, A. G. 1970, *Radio astrophysics. Nonthermal processes in galactic and extragalactic sources*, ed. Pacholczyk, A. G.
- Pedlar, A., Kukula, M. J., Longley, D. P. T., Muxlow, T. W. B., Axon, D. J., Baum, S., O’Dea, C., & Unger, S. W. 1993, *MNRAS*, 263, 471
- Pringle, J. E. 1996, *MNRAS*, 281, 357
- Randall, S. W., Forman, W. R., Giacintucci, S., Nulsen, P. E. J., Sun, M., Jones, C., Churazov, E., David, L. P., Kraft, R., Donahue, M., Blanton, E. L., Simionescu, A., & Werner, N. 2010, *ArXiv e-prints* (1006.4379)

- Reynolds, C., Punsly, B., Kharb, P., O’Dea, C. P., & Wrobel, J. 2009, *ApJ*, 706, 851
- Roy, A. L., Ulvestad, J. S., Wilson, A. S., Colbert, E. J. M., Mundell, C. G., Wrobel, J. M., Norris, R. P., Falcke, H., & Krichbaum, T. 2000, in *Perspectives on Radio Astronomy: Science with Large Antenna Arrays*, ed. M. P. van Haarlem, 173
- Sadler, E. M., Slee, O. B., Reynolds, J. E., & Roy, A. L. 1995, *MNRAS*, 276, 1373
- Sanders, R. H. 1982, in *IAU Symposium, Vol. 97, Extragalactic Radio Sources*, ed. D. S. Heesch & C. M. Wade, 145–147
- Schinnerer, E., Eckart, A., & Boller, T. 2000, *ApJ*, 545, 205
- Sharp, R. G., & Bland-Hawthorn, J. 2010, *ApJ*, 711, 818
- Smith, M. D., & Norman, C. A. 1981, *MNRAS*, 194, 771
- Sternberg, A., & Soker, N. 2008, *MNRAS*, 384, 1327
- Taylor, D., Dyson, J. E., & Axon, D. J. 1992, *MNRAS*, 255, 351
- Thean, A., Pedlar, A., Kukula, M. J., Baum, S. A., & O’Dea, C. P. 2000, *MNRAS*, 314, 573
- Tremblay, G. R., O’Dea, C. P., Baum, S. A., Koekemoer, A. M., Sparks, W. B., de Bruyn, G., & Schoenmakers, A. P. 2010, *ApJ*, 715, 172
- Ulvestad, J. S., Antonucci, R. R. J., & Barvainis, R. 2005, *ApJ*, 621, 123
- Ulvestad, J. S., Roy, A. L., Colbert, E. J. M., & Wilson, A. S. 1998, *ApJ*, 496, 196
- Ulvestad, J. S., & Wilson, A. S. 1984, *ApJ*, 285, 439
- Urry, C. M., & Padovani, P. 1995, *PASP*, 107, 803
- Veilleux, S., & Bland-Hawthorn, J. 1997, *ApJ*, 479, L105
- Veilleux, S., Tully, R. B., & Bland-Hawthorn, J. 1993, *AJ*, 105, 1318
- Weedman, D. W. 1983, *ApJ*, 266, 479
- Wehrle, A. E., & Morris, M. 1988, *AJ*, 95, 1689
- Wilson, A. S. 1981, in *ESA Special Publication, Vol. 162, Optical Jets in Galaxies*, ed. B. Battrick & J. Mort, 125–130



- Wilson, A. S., Shopbell, P. L., Simpson, C., Storch-Bergmann, T., Barbosa, F. K. B., & Ward, M. J. 2000, *AJ*, 120, 1325
- Wilson, A. S., & Ulvestad, J. S. 1982, *ApJ*, 263, 576
- Wilson, A. S., Yang, Y., & Cecil, G. 2001, *ApJ*, 560, 689
- Wong, K., Sarazin, C. L., Blanton, E. L., & Reiprich, T. H. 2008, *ApJ*, 682, 155
- Zurita, A., Rozas, M., & Beckman, J. E. 2000, *A&A*, 363, 9

Table 1. Source Parameters at 1.6 GHz

Comp.	Peak Intensity	Total Intensity	Position R.A., Decl.	Angular Separation	Linear Separation
1	$0.46 \pm 0.09$	$0.50 \pm 0.18$	19h 08m 16.4322s, $50^\circ 55' 59.526''$	....	....
2	$0.35 \pm 0.09$	$0.40 \pm 0.16$	19h 08m 16.4320s, $50^\circ 55' 59.522''$	$4.3''$	0.7
3	$0.23 \pm 0.09$	$0.30 \pm 0.20$	19h 08m 16.4325s, $50^\circ 55' 59.532''$	$6.1''$	0.9

Note. — Column 1: component number. Columns 2 and 3: peak and integrated intensity in  $\text{mJy beam}^{-1}$ . Column 4: position of components in sky. Columns 5 and 6: the angular and linear projected separation between components 2 and 3 with respect to component 1, in arcseconds and parsecs, respectively.

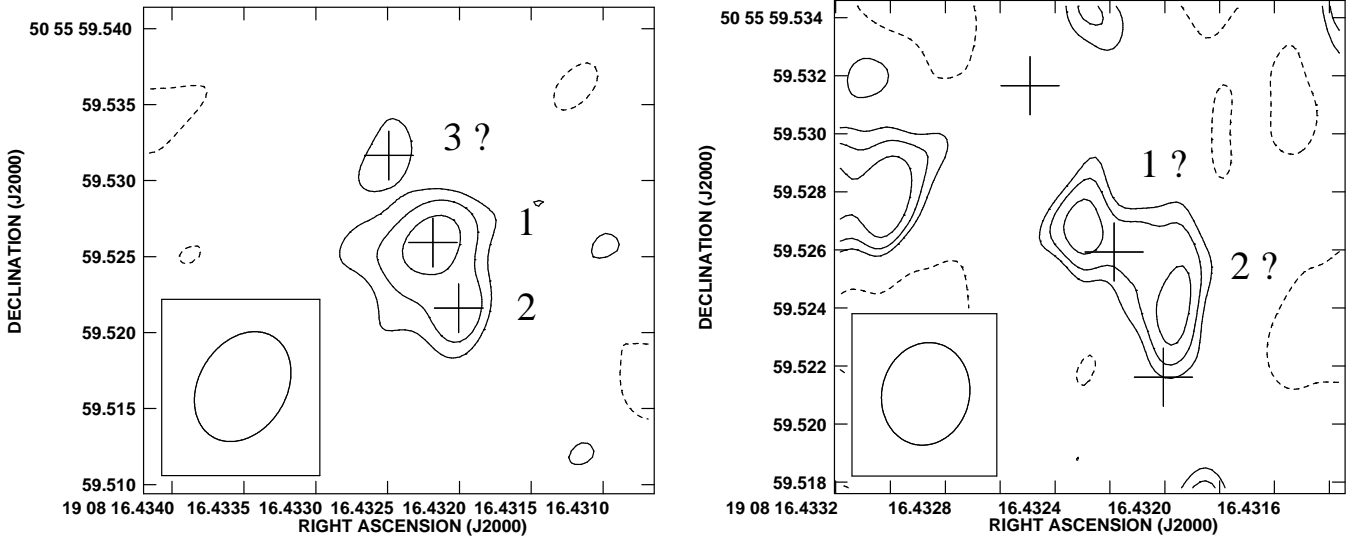


Fig. 1.— 1.6 GHz (left) and 4.9 GHz (right) surface brightness contour maps of the parsec-scale structure in NGC 6764. The contours are (left)  $\pm 0.18, 0.26, 0.37 \text{ mJy beam}^{-1}$ , and (right)  $\pm 0.09, 0.13, 0.18 \text{ mJy beam}^{-1}$ . We identify the components 1, 2, and 3, to be the core, jet, and a *possible* counterjet. The peak positions of the three components observed at 1.6 GHz have been marked with crosses in both the panels.

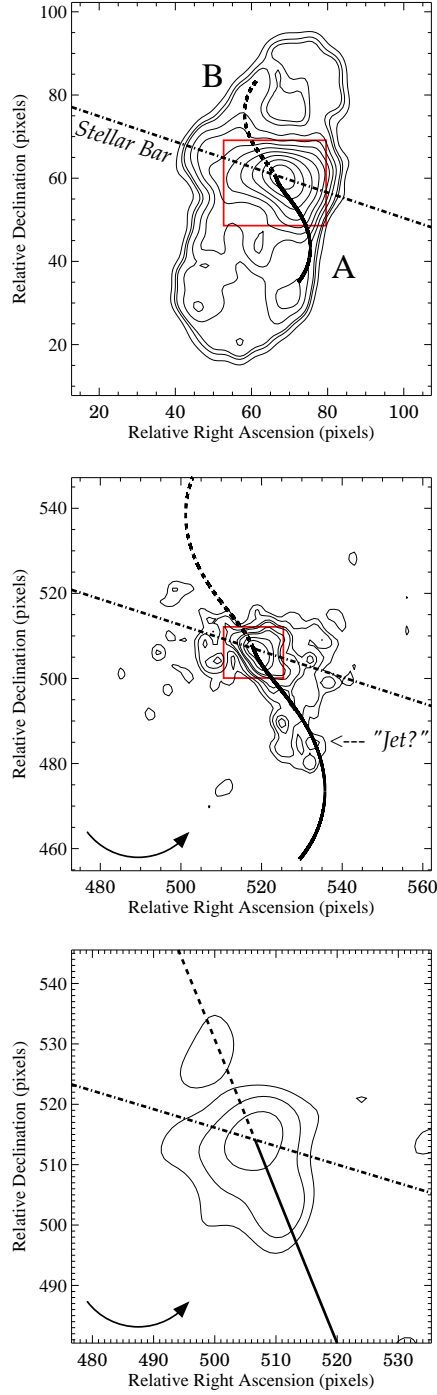


Fig. 2.— Precessing jet model can be fitted to the radio emission from parsec- to sub-kpc scales. (top) VLA A-array 1.4 GHz image (pixel size =  $0.2'' = 31$  pc); (middle) VLA A-array 4.86 GHz image (pixel size =  $0.1'' = 15.4$  pc); and (bottom) VLBA image at 1.6 GHz (pixel size =  $0.4$  mas =  $0.06$  pc). The peak radio emission is at R.A. = 19h 08m 16.432s, decl. = 50d 55m 59.525s. The red box indicates the region zoomed in on the panel below, while the curved arrow indicates the sense of the galaxy rotation. Image contour levels are (top) 0.25, 0.4, 0.5, 0.8, 1.13, 1.6, 2.25, 3.2, 4.5, 6.4, 9.0 mJy beam $^{-1}$ , (middle) 0.08, 0.125, 0.2, 0.25, 0.4, 0.5, 0.8, 1.12, 1.6, 2.25, 3.2, 4.5, 6.4 mJy beam $^{-1}$ , and (bottom) 0.18, 0.26, 0.37 mJy beam $^{-1}$ .